Where does atomic photoionization begin?

I. A. Ivanov* and A. S. Kheifets
Research School of Physical Sciences, The Australian National University, Canberra ACT 0200, Australia
(Dated: September 1, 2011)

We perform a time-delay analysis of of strong field ionization of atomic hydrogen in the tunnelling regime. We obtain the values of the time delay from the quantum-mechanical calculation involving solution of the time-dependent Schrödinger equation, and use these values as parameters defining corresponding classical trajectories. We demonstrate that almost all the classical trajectories, defined by this procedure, tend to cluster together to a few starting points. This allows one to pose sensibly and answer the question as to when and where the atomic photoionization process actually begins.

PACS numbers: 32.30.Rj, 32.70.-n, 32.80.Fb, 31.15.ve

Presently available experimental techniques such as attosecond streaking [1, 2] and angular attosecond streaking (attoclock) [3, 4] make it possible to trace electronic motion in atoms and molecules with the resolution of several attoseconds. This allows one to pose, and answer experimentally, questions which would have seemed rather scholastic merely a decade ago. One such a question, which has recently drawn considerable attention, is *when does atomic photoionization begin?* [5]. This question was first raised after experimental observation of a noticeable time delay between photoelectrons emitted from the $2s$ and $2p$ shells in neon [6]. Later, a similar observation was reported of the time delay between the $3s$ and $3p$ photoelectrons in argon [7]. The experimental time delay investigations [6, 7] and the subsequent theoretical works [8, 9, 10, 11, 12] were restricted to the XUV photon energy range and the so-called multiphoton ionization regime. This regime is characterized by the values of the Keldysh parameter $\gamma \gg 1$, where $\gamma = \omega\sqrt{2I_{\rm p}}/F$ with $I_{\rm p}$ being the atomic ionization potential, F and ω being the strength and angular frequency of the laser field. The alternative regime of tunneling ionization in the NIR photon energy range with $\gamma < 1$ was investigated by Eckle *et al* [3, 4] who determined experimentally the time needed for an electron to tunnel out of the atom.

In the present Letter, we also consider the tunneling ionization regime and generalize the time-delay theory for this problem. We are motivated by the following consideration. The concept of a time delay, as defined by the wave packet back propagation [6, 8], gives us information about a certain combination of the initial time and initial coordinate for the trajectory which the center of the ionized wavepacket follows. Assuming a straight line asymptotics of this trajectory at large times and distances and back propagating it to the origin, we can define the time delay as $\Delta \simeq t_0 - r_0/v$, where v is the velocity of the center of the outgoing wavepacket, t_0 is the moment of time when this wavepacket has been formed and r_0 is the coordinate of this event. We recall that for the tunneling ionization regime t_0 is precisely known. As it follows from the well-known and tested classical model of tunneling ionization [13], the electron velocity gained in the EM field is determined by the value of the vector potential $A(t_0)$ at the moment of ionization, an observation which lies at the heart of the attosecond streaking technique. We have means, therefore, to determine experimentally t_0 and then, knowing the time-delay, to define unamiguosly r_0 - the initial coordinate of the electron at the moment of ionization. Below, we explore this idea more rigorously and present some numerical results. The atomic units are used throughout the paper unless specified otherwise.

We consider photoionization process in the hydrogen atom driven by a laser pulse. We will use below both classical and quantum descriptions of the electron motion for times long after the end of the laser pulse. To simplify our analysis, we consider experimental geometry in which detectors are placed so that electrons moving in forward direction with asymptotic velocity v parallel to the z-axis and impact parameter R are detected at very large times. Asymptotic description of the classical electron trajectories, satisfying the conditions above, can be obtained from the Newton equations of motion in the Coulomb field. Due to the axial symmetry of the problem, we can consider electron motion in a plane, which we choose to be the (x, z) plane. For large time $t \to \infty$, we can write the solution of the equations of motion as

$$\ddot{x} = -\frac{x}{(x^2+z^2)^{3/2}} \quad , \quad \ddot{z} = -\frac{z}{(x^2+z^2)^{3/2}}, \qquad (1)$$

This solution satisfies the asymptotic expansions

$$x \approx x_1 = R \quad , \quad z \approx vt + \frac{\ln t}{v^2} + c \; , \qquad (2)$$

where we omitted terms of the order of t^{-1}. Asymptotic motion is thus determined by the impact parameter R and the constant c, the latter being undefined in a classical description.

To proceed further, we turn to the quantum mechanical treatment. We solve the time dependent Schrödinger equation (TDSE) for the hydrogen atom driven by a laser pulse with the electric field directed along the z axis and

*Corresponding author: igor.ivanov@anu.edu.au

defined for $t \in (-2T, 2T)$ as:

$$F(t) = F_0 \cos^2\left(\frac{\pi t}{4T}\right) \cos\omega t \ . \tag{3}$$

Here the base frequency $\omega = 0.0577$ a.u. (corresponding to the wavelength $\lambda = 790$ nm), $F_0 = 0.1068$ a.u. (corresponding to the peak intensity of 10^{14} W/cm^2 and $T = 2\pi/\omega = 2.63$ fs is the optical cycle for the base frequency ω. These values define the Keldysh parameter $\gamma = 0.53$. The field is zero outside the interval $(-2T, 2T)$, the total duration of the pulse is thus $4T \approx 10.5$ fs. At the moment of time $t = -2T$, the hydrogen atom is initially in the ground state. To describe electromagnetic (EM) interaction, we use the velocity gauge: $\hat{H}_{\rm int}(t) = \boldsymbol{A}(t)\cdot\hat{\boldsymbol{p}}$, with $\boldsymbol{A}(t) = -\int_{-2T}^{t} \boldsymbol{F}(\tau)\, d\tau$ and the electric field $\boldsymbol{F}(t)$ described above. The time dependence of $F(t)$ and $A(t)$ is visualized on the left panel of Fig. 1.

To solve the TDSE, we employ the computational procedure employed in our previous work [14]. Numerically, the TDSE is discretized on the grid with the stepsize $\delta r = 0.05$ a.u. in a box of the size $R_{\rm max} = 1500$ a.u. We seek a solution of the TDSE on the basis of a partial wave expansion

$$\Psi(\boldsymbol{r}, t) = \sum_{l=0}^{r_{\rm max}} f_l(r, t) Y_{l0}(\theta) \ , \tag{4}$$

where summation is restricted to $l_{\rm max} = 20$. It is known [15], that our numerical choices are sufficient to achieve convergence with respect to the number of partial waves. To propagate the wave-function (4) on the interval $(-2T, 2T)$, we use the matrix iteration method developed in Ref. [16].

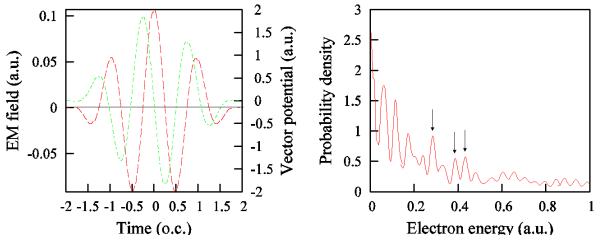

FIG. 1: (Color online) Left panel: the electric field (red) and vector potential (green) of the laser pulse. Right panel: the photoelectron energy spectrum. The arrows indicate selected photoelectron energies used for timing analysis below.

We expand the solution of the TDSE at the moment $t \geq T_1 = 2T$ on the set of the Coulomb functions (with ingoing boundary conditions)

$$\Psi(t) = \int a(\boldsymbol{k}) \phi^-_{\boldsymbol{k}} e^{-iE_k t}\, d\boldsymbol{k} \ . \tag{5}$$

The expansion coefficients $a(\boldsymbol{k})$ determine various ionization probabilities, in particular, the photoelectron energy spectrum as shown on the right panel of Fig. 1. More importantly for our purposes, the coefficients $a_{\boldsymbol{k}}$ can be used to study large time behavior of a wavepacket corresponding to the particular detection geometry. The wavepacket describing electrons propagating along the z-axis with particular value of the velocity v and a given value of the impact parameter R can be obtained from the solution $\Psi(t)$ by means of two projection operators, or two "measurements". The one projection restricts the range of momentum integration in Eq. (5) to some neibourhood of $\boldsymbol{v}$, where $\boldsymbol{v}$ is directed along the z-axis. Another projection restricts the wave function in the perpendicular (x, y) plane to a neibourhood of the point $\boldsymbol{\rho}$ in this plane such that $\rho = R$. In the case of an ideal (or a von Neumann measurement), this second operation consists in putting the wave function to zero for all $\boldsymbol{\rho}$ outside this neibourhood in the (x, y) plane and leaving it unchanged for the $\boldsymbol{\rho}$ values inside. For the large time, when the "measurements" are performed, we can write such a wavepacket as

$$\tilde{\Psi}(t) = \int_{\Omega} a_{\boldsymbol{k}} \phi^-_{\boldsymbol{k}} f(\boldsymbol{\rho}, t) e^{-iE_k t}\, d\boldsymbol{k} \ , \tag{6}$$

where Ω is a region in the momentum space containing the point $\boldsymbol{k} = \boldsymbol{v}$, and the function $f(\boldsymbol{\rho}, t)$ may spread in time in the (x, y) plane, but remains peaked at the point in the (x, y) plane corresponding to a given impact parameter. Particular values of the velocity v the region Ω in the momentum space defining integration in Eq. (6) were chosen as follows. We analyze absolute values of the coefficients $a(\boldsymbol{k})$, with $\boldsymbol{k} = (0, 0, k_z)$, as a function of k_z. This function follows closely the pattern shown on the right panel of Fig. 1 which consist of a series of local maxima with energies separated by the base frequency ω. We take such a local maximum $k_z = v$ as the center of the wavepacket and restrict integration in k_z in Eq. (6) to $(k_z \in \sqrt{v^2 - \omega}, \sqrt{v^2 + \omega})$. Thus we obtain wavepackets which physically represent electrons contributing to a given peak of the spectrum of above threshold ionization (ATI) and move in the forward direction.

We are interested in the motion of the center of this wavepacket and in matching it to the classical asymptotics in Eq. (2). Similarly to our classical calculation, we can assume that this motion occurs in the (x, z) plane. From Eq. (6) we see that the asymptotic equation for the x- coordinate is satisfied automatically. Asymptotic equation for the z-coordinate can be obtained using the saddle-point method and the asymptotic form $\phi^-_{\boldsymbol{k}} \propto e^{i\boldsymbol{kr} + i\gamma(\boldsymbol{r}, \boldsymbol{k})}$, with $\gamma(\boldsymbol{r}, \boldsymbol{k}) = k^{-1} \ln(kr + \boldsymbol{kr})$ for the hydrogen scattering states [17, 18].

By writing explicitly notation $a_{\boldsymbol{k}} = |a_{\boldsymbol{k}}| e^{i\delta}$, we obtain the following asymptotic equation for the z-coordinate of the center of the wavepacket given by Eq. (6):

$$z \approx v\left(t - \frac{\partial\delta}{\partial v}\frac{1}{v}\right) + \frac{\ln t}{v^2} + \frac{\ln 2v^2 - 1}{v^2} \tag{7}$$

The quantity $\Delta = \dfrac{\partial\delta}{\partial v}\dfrac{1}{v}$ can be interpreted as the Wigner time delay [17, 18]. By comparing the classical and quan-

tum asymptotics, we find relation between the constant c in Eq. (2) and the time-delay in Eq. (7).

Knowing the TDSE solution (6), we can determine values of the time delay for various wavepacket center energies and particular geometry. Thus, we can determine values of the parameter c in the asymptotic classical equation (2) for the z-coordinate. This leaves us with one undetermined parameter x_1 in the equation for the x-coordinate. For different values of the parameter x_1, we can use asymptotic equations (2) for sufficiently large $t = t_f$ (in the calculation we used $t_f = 50,000$ a.u.) to compute values of x and z coordinates at $t = t_f$. Together with the known values of the x- and z- components of the velocity, these values provide us with the initial (or rather final) conditions. Propagating classical equations of motion of an electron in the Coulomb field and the field of the laser pulse defined in Eq. (3) backward in time (we employ the leap-frog method for this purpose), we obtain a one-parameter family of the classical electron trajectories. This family has the property, that all these trajectories have the same large-t asymptotic for the z-coordinate, coinciding with the quantum-mechanical asymptotic equation describing motion of the wavepacket center.

Not all of these trajectories are relevant though. From the Keldysh theory of tunneling ionization [19] and its refinement [20], we know that the electron velocity at the moment of ionization is small, large velocities are heavily (exponentially) dampened. To single out the trajectories possessing this property from our one-parameter family, we trace the velocity along the trajectory and look for the minima of its absolute value. If all the minima on a given trajectory exceed a certain value $v_{\max} = 0.2$ a.u., we discard such a trajectory. We can also expect that the electron should not emerge too far from the nucleus at the moment of ionization. Therefore, we also discard the trajectories for which there are minima with absolute value of the velocity less than $v_{\max}$, but the corresponding absolute value of the z-coordinate is greater than some $z_{\max} = 12$ au. Particular numerical values of $v_{\max}$ and $z_{\max}$ are not important, their role is merely to discard the classical trajectories which most strongly violate our selection criteria. For each classical trajectory which was sieved through these selection criteria, we obtain a point t_0, where the minimum of the absolute value of the velocity was attained, and corresponding values of $x_0 = x(t_0)$ and $z_0 = z(t_0)$. It is natural to interpret t_0 as the moment of time at which ionization occurs whereas x_0 and z_0 define the spatial coordinates of this event.

To illustrate our findings, we select several peak photoelectron energies $E = 0.283$ a.u., 0.391 a.u., and 0.435 a.u. which are marked by arrows on the right panel of Fig. 1. The time delay figures obtained from the TDSE solution are $\Delta = 537$ as, 435 as and 375 as, respectively. The corresponding values of $x(t_0)$ and $z(t_0)$ are plotted in Fig. 2. Upon inspection of this figure, it becomes immediately obvious that almost all the trajectories, which satisfy the tunneling ionization criteria, start at about the same moment $t_0 \simeq 0.4T$ with the initial values z_0 distributed very sharply. This indicates that our interpretation of t_0 and z_0 as the time and initial z-coordinate of the ionization event may be a meaningful one. There is a second family of the classical trajectories with larger value of z_0 for the energy of 0.391 a.u. (middle row in Fig. 2). This, we believe, is an artifact, introduced by our selection procedure. We could get rid of this family by reducing the parameter $z_{\max}$ from 12 a.u. to 8 a.u. in our selection criterion.

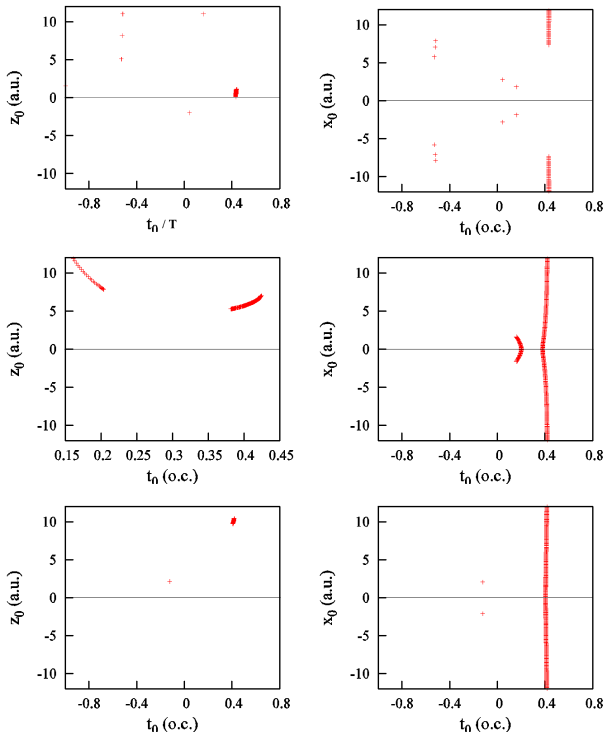

FIG. 2: (Color online) Distributions of initial values $z_0 = z(t_0)$ (left column) and $x_0 = x(t_0)$ (right column) for classical trajectories corresponding to photoelectrons moving in forward direction with energies $E = 0.283$ a.u. (upper row), 0.391 .u. (middle), and 0.435 a.u. (lower row).

We note further that the value of t_0, which we interpret as the moment when photoionization "begins", agrees well with what one would expect on the basis of the classical model [13]. This model predicts that the photoelectron velocity gained in the EM field is determined by the value of the vector potential $A(t_0)$ at the moment of ionization. From Fig. 1 we observe that $A(t_0 \simeq 0.4T) \approx 1$ a.u. which falls into the range of the final velocities we presently consider (from 0.75 a.u. to 0.93 a.u.).

As far as the z_0 coordinate is concerned, an estimate for this quantity could be obtained using a simple model illustrated in Fig. 3. Here we plot an effective potential $-1/z + F_{\rm eff} z$ as a function of the z-coordinate with $F_{\rm eff} \approx -0.08$ a.u. which is the value of the electric field (3) at the moment $t_0 \approx 0.4T$ when the ionization event

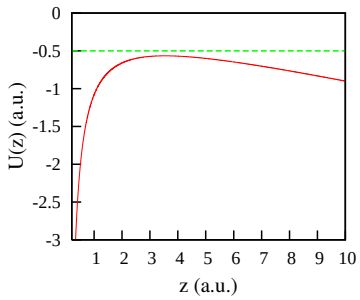

FIG. 3: (Color online) (Red) solid line: effective potential $-1/z + F_{\rm eff}z$ as a function of z-coordinate; (green) dashed line: $1s$ energy level of the atomic hydrogen $E = -0.5$ a.u.

occurs. The figure illustrates the case of the over the barrier ionization, and we can estimate z_0 as the coordinate of the maximum of $U(z)$ which is $|F_{\rm eff}|^{-1/2} \approx 3.5$ a.u. This simple estimate supports qualitatively our findings. However, it does not capture some additional features seen in Fig. 2 such as growth of z_0 with electron energy. This growth can be explained in the following way. As a rough approximation, we can picture electron motion in the z-direction as a straight line. In this approximation, the value of the z-coordinate at the moment of ionization is $z_0 = v(t_0 - \Delta)$, where Δ is the time delay. which decreases with energy. If we plug the values of the time delay reported above into this formula together with $t_0 \approx 0.4T$, we obtain $z_0 = 16.5$ a.u., 23.1 a.a., and 26.7 a.u. for the energies of 0.283 a.u., 0.391 a.u., and 0.435 a.u. respectively. The absolute values of z_0 derived from the straight line trajectories are inaccurate because of a crude character of this approximation. However, these values demonstrate the same characteristic increase with energy as is seen in Fig. 2.

Plots for the initial values of the x- coordinate are less informative. They tell us again that trajectories start at $t_0 \approx 0.4$. The only exception is the plot in the middle row of Fig. 2. On this plot, the second family of the trajectories with larger z_0 can be removed if we made the $z_{\rm max}$ selection criteria more stringent.

To conclude, we establish the defining moment of atomic ionization when the photoelectron leaves the atom. This moment is mapped distinctively on the coordinate space which allows one to speculate as to *where atomic photoionization actually begins*. As always, when trying to describe a quantum-mechanical phenomenon using the classical language, we have to rely on some classical tool. In this work, such a tool is the classical trajectory analysis using an additional information on the time delay supplied by the quantum-mechanical TDSE calculation. As a result of this procedure, we define the moment of ionization t_0 which agrees well with what one would expect from the purely classical model [13]. Success of the latter model in describing such phenomena as ATI, multiphoton two-electron ejection or high harmonic generation tells us that classical concepts, such as the moment the ionization event, may be extremely useful. In the present work, we introduced rigorously another such a concept: the localization of the ionization event in space. We hope this localization may be determined experimentally in future attosecond experiments.

[1] A. Baltuska *et al*, *Attosecond control of electronic processes by intense light fields*, Nature **421**, 611 (2003).

[2] R. Kienberger *et al*, *Atomic transient recorder*, Nature **427**, 817 (2004).

[3] P. Eckle *et al*, *Attosecond angular streaking*, Nat. Phys. **4**, 565 (2008).

[4] P. Eckle *et al*, *Attosecond ionization and tunneling delay time measurements in helium*, Science **322**(5907), 1525 (2008).

[5] H. W. van der Hart, *When Does Photoemission Begin?*, Science **328**(5986), 1645 (2010).

[6] M. Schultze *et al*, *Delay in Photoemission*, Science **328**(5986), 1658 (2010).

[7] K. Klünder *et al*, *Probing single-photon ionization on the attosecond time scale*, Phys. Rev. Lett. **106**(14), 143002 (2011).

[8] A. S. Kheifets and I. A. Ivanov, *Delay in atomic photoionization*, Phys. Rev. Lett. **105**(23), 233002 (2010).

[9] A. S. Kheifets, I. A. Ivanov, and I. Bray, *Timing analysis of two-electron photoemission*, J. Phys. B **44**(10), 101003 (2011).

[10] I. A. Ivanov, *Time delay in strong-field photoionization of a hydrogen atom*, Phys. Rev. A **83**(2), 023421 (2011).

[11] S. Nagele *et al*, *Time-resolved photoemission by attosecond streaking: extraction of time information*, J. Phys. B **44**(8), 081001 (2011).

[12] L. R. Moore *et al*, *Time delay between photoemission from the 2p and 2s subshells of Neon atoms* (2011). In XXVII ICPEAC.

[13] P. B. Corkum, *Plasma perspective on strong field multiphoton ionization*, Phys. Rev. Lett. **71**, 1994 (1993).

[14] I. A. Ivanov, *Modifying the high-energy part of the above-threshold-ionization spectrum*, Phys. Rev. A **82**(3), 033404 (2010).

[15] A. N. Grum-Grzhimailo *et al*, *Ionization of atomic hydrogen in strong infrared laser fields* Phys. Rev. A **81**(4), 043408 (2010).

[16] M. Nurhuda and F. H. M. Faisal, *Numerical solution of time-dependent Schrödinger equation for multiphoton processes: A matrix iterative method*, Phys. Rev. A **60**(4), 3125 (1999).

[17] E. P. Wigner, *Lower limit for the energy derivative of the scattering phase shift*, Phys. Rev. **98**(1), 145 (1955).

[18] C. A. A. de Carvalho and H. M. Nussenzveig, *Time delay*, Phys. Rep. **364**(2), 83 (2002).

[19] L. V. Keldysh, *Ionization in the field of a strong electromagnetic wave*, Sov. Phys. JETP **20**, 1307 (1965).

[20] A. M. Perelomov and V. S. Popov, *Atomic ionization in time-varying electric field*, Sov. Phys. JETP **25**, 482 (1967).